

INFLUENCE ANALYSIS OF THREE DIFFERENT CAMERA CALIBRATION METHODS ON A CAMERA-PROJECTOR MEASURING SYSTEM

Julieta Tiscareño Félix, José Antonio Albajez García, Jorge Santolaria Mazo

UNIVERSITY OF ZARAGOZA. Design and Manufacturing Engineering Department - María Luna, 3 (Building Torres Quevedo) 50018 Zaragoza

DOI: <https://doi.org/10.6036/10796> | Received: 27/jan/2022 • Reviewing: 17/may/2022 • Accepted: 17/oct/2022

To cite this article: INFLUENCE ANALYSIS OF THREE DIFFERENT CAMERA CALIBRATION METHODS ON A CAMERA-PROJECTOR MEASURING SYSTEM. TISCAREÑO-FÉLIX, Julieta; ALBAJEZ-GARCÍA, José-Antonio; SANTOLARIA-MAZO, Jorge. DYNA. March - April 2024, vol. 99, n.2, pp. 195-200. DOI: <https://doi.org/10.6036/10796>

ABSTRACT:

The challenges arising from mass production with high quality level require advanced error measurement systems and optical metrology systems. Nowadays, it is more frequent to find this type of controls at the manufacturing industry into the quality control procedures as long as the need for a faster capture speed and precision has increased. However, these techniques can be improved. The accuracy of 3D measurement systems formed by a camera-projector pair depends directly on the calibration procedure used. The projector is usually modelled as the inverse projection of a pin-hole camera, which presents the option to calibrate the system by two different approaches: as a whole system or separately. The most common approach is the use of a camera previously calibrated, followed by the calibration of the projector. Studies show that the uncertainty of the camera parameters from its calibration propagates to the projector parameters and several authors conclude that the three most widespread are: Tsai, Zhang and Direct Linear Calibration. The objective of this study is to have a clear comprehension of the relationships between the camera and projector parameters and of how uncertainty is propagated to the measurement system error. Therefore, the three calibration methods previously mentioned and some of them possible combinations are analyzed.

Keywords: Quality Control; Projector-camera calibration; Error propagation; Measurement System Error.

FUNDING

This work was supported by project "T56_23R: GIFMA. Grupo de ingeniería de fabricación y metrología avanzada" funded by Gobierno de Aragón.

1.- INTRODUCTION

The challenges arising from large-scale, high-quality production requiring increasingly advanced error measurement systems and optical metrology systems (including laser, photogrammetry and white light projection), are becoming more important. The scanning of three-dimensional objects has become a quality control procedure commonly used in the industry due to the levels of precision achieved and its high speed of capture, however techniques can still be improved. To improve the general quality of these techniques,

different measurement configurations [1] and more precise algorithms [2] are being sought. Therefore, identifying the cause of the results not meeting expectations is a complicated and slow task, but with great interest.

Currently, 3D measurement systems are widely applied in industrial metrology, medicine, cultural heritage and other areas [3-13]. Besides their fast speed and noncontact nature, many of those applications require considerable measurement accuracy. For that reason, it is important to study and improve this kind of systems to have as much information as possible.

Nowadays, there is a wide variety of measuring equipment based on active stereometric systems; those formed by one or more cameras and an element that acts as an active emitter, usually of two types: laser [14-16] or structured light [17-19]. In the case of 3D measurement systems formed by a camera-projector pair, their accuracy depends to some extent on the accuracy of the calibration of the whole measurement system.

Single camera calibration has been extensively studied and numerous calibration methods have been proposed [20-23]. Studies have been conducted from overall reviews [24] and general investigations [25] to parameter stability [26-27], even the feasibility of using low-cost camera has been analyzed [27-29]. Camera calibration can be classified according to several different criteria: Linear or non-linear calibration, intrinsic or extrinsic calibration, implicit or explicit calibration, point-based or line-based methods, or a combination of them [30].

The mathematical model of the pin-hole camera [31] is widely used; its objective is to find a linear relationship between the 3D points of the scene with their 2D projection points in the image plane. Suppose a 3D point Q_w in the world coordinate system with its homogenous coordinates on the world plane $(X_w, Y_w, Z_w, 1)$, is projected to a point Q_c , $(x, y, 1)$, in the image plane of the camera with coordinates x and y . Then according to the pin-hole camera model,

$$Q_c = sM_c(R_c \ T_c)Q_w \quad (1)$$

where 's' is the scale factor and M_c is the set of camera intrinsic parameters given as,

$$M_c = \begin{pmatrix} f_x & 0 & C_x \\ 0 & f_y & C_y \\ 0 & 0 & 1 \end{pmatrix} \quad (2)$$

The parameters (C_x, C_y) are the co-ordinates of the principal focus and f_x and f_y are the focal lengths of the x and y axes of the image plane respectively.

$[R_c \ T_c]$ represents the transformation matrix, extrinsic parameters.

$$[R_c \ T_c] = \begin{pmatrix} r_{11} & r_{21} & r_{31} & t_x \\ r_{12} & r_{22} & r_{32} & t_y \\ r_{13} & r_{23} & r_{33} & t_z \end{pmatrix} \quad (3)$$

It gives the rotation and translation between the world coordinate system and camera planes.

Several authors conclude that the three most widespread camera calibration procedures are: Tsai, Zhang and Direct Linear Calibration (DLC) [32-34]. Tsai is a multiple viewing position method based on the model of the pin-hole camera; this model transforms points in the world reference frame (X_w, Y_w, Z_w) to points in the frame of image reference (u, v) and considers radial distortion. Zhang also uses traditional calibration techniques (known calibration points) and self-calibration techniques (correspondence between calibration points when they are in different positions). Moreover, this method considers and compensates three distortion types: radial, decentering and thin prism distortion. DLC ignores the lens distortion and it is based on the co-linearity between a point expressed in the world reference system (x, y, z) , its directly equivalent in the image reference coordinates (u, v) and the central projection point of the camera [32]. On one hand, the comparison of these methods shows their advantages and disadvantages in different situations [33-34]. On other hand, there are studies that are focused on how distortions affect the results [30,35].

When a projector is included in the system, it is usually modelled as an inverse camera because it works fundamentally like a pin-hole reverse camera, projecting an image instead of capturing it [36]. Therefore, it is possible to calibrate it with any conventional camera calibration method. This presents the option to calibrate the system by two different approaches: as a whole system or separately. The most common approach is the use of a camera previously calibrated, followed by the calibration of the projector, using the DLC method, with this camera. Nevertheless, studies show that this method propagates the uncertainty from the camera calibration procedure to

the projector [37], and consequently the importance of the camera calibration increases. Authors have analyzed the system sensitivity to different factors in a rigid configuration, using only the DLC method in both calibrations (camera and projector), and have verified the effect of the errors on the lens distortion parameters and extrinsic parameters, concluding that the first ones have the greatest impact [38].

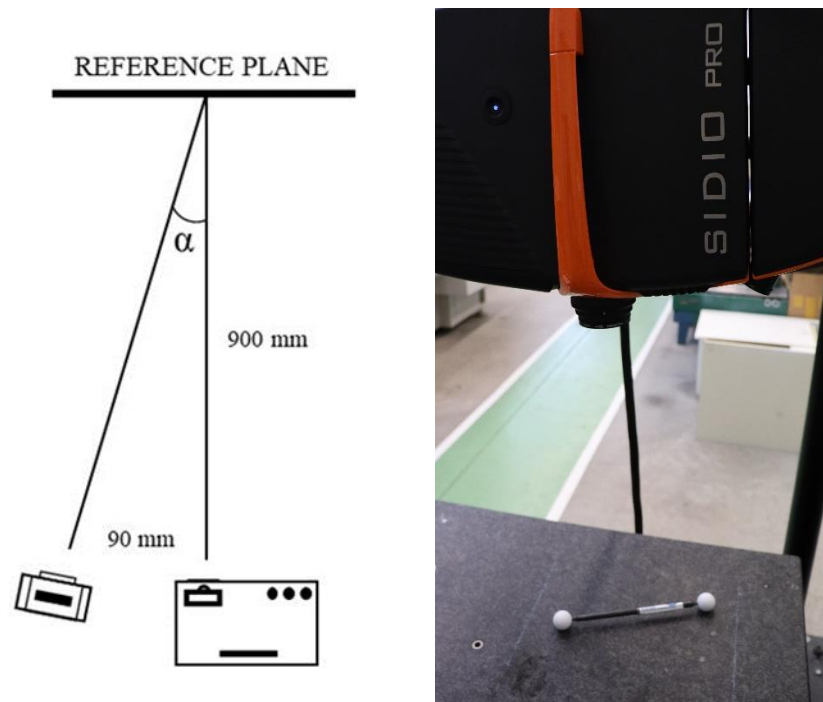
Considering the crucial role that camera calibration has for the total system calibration, it was decided to simulate the camera calibration by Tsai, Zhang and DLC methods to have a clearer vision of how camera parameters and measurement errors are affected. For the projector, it was decided to simulate a perfect one using perfect calibration points to appreciate only the influence of the camera on it. Based on this, the DLC method was selected for two reasons: 1) The simplicity of the algorithm allows to see more clearly the propagation to the projector; 2) The iterative procedure that the DLC method uses allows you to obtain very good results, if it is allowed to converge and time limit to calculate an optimal solution and, computational cost is not determining factors in this study. The objective of this study is to provide two contributions: from a general point of view, to obtain a better understanding of the relationships among the camera and projector parameters, and how uncertainty propagates from the camera to the projector. Specifically, the comparison of the three configurations (camera calibration by DLC, Tsai and Zhang, and projector calibration by DLC) as well as the advantages and disadvantages of each of them and how to compensate them.

2.- MATERIALS AND METHODS

It was decided to use simulations for the analysis of this study since these allow us to isolate the specific error selected. In our case, it is how uncertainty propagates from camera to projector and consequently to the whole measurement system.

The synthetic experiment based on the Monte Carlo method simulated the calibration of a measurement system formed by a camera-projector pair separately. Firstly, the camera was calibrated by three different methods: DLC, Tsai and Zhang, then the projector was calibrated, using that camera, by the DLC method. In each of these configurations, 5000 simulations were performed in order to analyze the factors that could influence the generation of uncertainty on the results. The number of simulations was decided on the basis of a convergence analysis, where an increasing number of Monte Carlo trials were performed until the various outcomes of interest were stabilized in a statistical sense. Figure 1 shows the camera-projector setup used. It was based on a measuring equipment owned by the Department of Design and Manufacturing Engineering of the University of Zaragoza: SIDIO Pro.

The camera data are 0.0067 mm for the pixel size dx and dy in X and Y axis respectively; 1280/2 for C_u and 1024/2 for C_v , corresponding to the center of the camera coordinates; 1280 for N_{cx} and N_{fx} , number of sensor elements in X axis of the camera (sels) and number of pixels in x direction of the frame grabber (pixel) respectively. The projector resolution was 1024x768, and the camera radial lens distortion coefficient was $k1=0.0015$. It was decided to include only radial distortion because this is the only distortion considered in two of the three methods applied, Tsai and Zhang.




| | | |
|---|--|--|
|  | <p style="text-align: center;">INFLUENCE ANALYSIS OF THREE DIFFERENT CAMERA CALIBRATION METHODS ON A CAMERA-PROJECTOR MEASURING SYSTEM</p> | <p style="text-align: center;">UNITS AND CONSTANTS</p> |
| <p style="text-align: center;">INVESTIGATION ARTICLE</p> | <p style="text-align: center;">Julieta Tiscareño Félix, José Antonio Albajez García, Jorge Santolaria Mazo</p> | <p style="text-align: center;">Metrology</p> |

Figure 1. Left: Measurement system setup. Right: Physical representation.

The factors selection was pre-selected from the characteristic parameters of the camera provided by the manufacturer in the typical technical sheet. Usually, manufacturers provide values accuracy in 4 decimals. For measurement purpose that give us a range equivalent to around 2% of the specified value.

The camera data will be referred to those parameters: dx, dy, Cu, Cv. Afterwards, the factors selection was determined by a preliminary mathematical analysis of the three calibration methods selected. This analysis consisted of a detailed review of the mathematical procedures behind each calibration method and how the camera data interacted with them.

On one hand, we could appreciate that the camera data corresponding to the pixel size (dx and dy) and the center of the camera coordinates (Cu and Cv) directly affect the calculation of the camera calibration intrinsic and extrinsic parameters in the DLC and Tsai methods.

On other hand, those camera data (dx and dy) only affect the focal length calculation (f) in the Zhang method. The robustness of this method prevents directly affecting most of the camera calibration intrinsic and extrinsic parameters calculation. In this case, the measurement error is affected mostly by extrinsic parameters and distortion calculation. For that reason, it was decided to introduce a $\pm 5\%$ error in the parameters that interfere in the calculation of the camera calibration extrinsic parameters and a radial lens distortion of Zhang method. A $\pm 5\%$ error was introduced in the parameters dx, dy, Cu and Cv for Direct Linear Calibration and Tsai methods. All these errors follow a normal Gaussian distribution without correlation over the selected parameters.

The case of no correlation has been considered to facilitate the interpretation of the output data by limiting the sources of variability in the input parameters. If some type of correlation had been considered, it would be a correlation value 1 between dx and dy. This correlation would imply that the pixel remains square. This is relevant because Tsai method considers dx and dy, while the DLT method only models dx.

3.- SIMULATION RESULTS

The first part of this section shows the behavior of the different parameters of the camera and the camera error measure, obtained by a Monte Carlo synthetic experiment in MATLAB. As an example, Figure 2 (a, b, c) shows the results of camera focal length calculation by the three different methods in function of camera dy. The camera focal center will be referred to the effective focal length of the pin-hole camera. It was decided to show the results of camera focal length calculation just in function of dy because in the case of TSAI method just take in account this parameter.

In this first parameter analyzed is possible to observe that the behavior of the three camera focal center calculations is essentially lineal and that the most affected focal center calculation is corresponded to the Direct Lineal Calibration method.

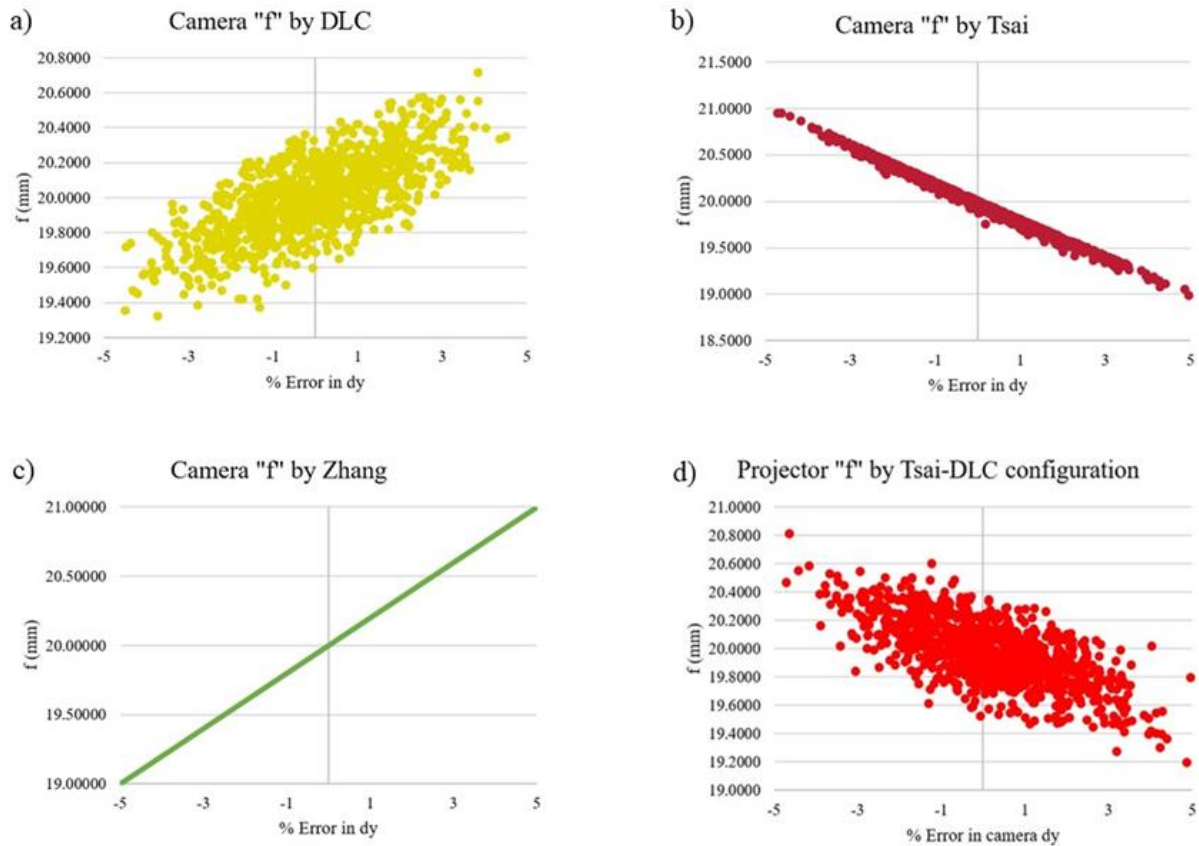


Figure 2. (a) Camera f by DLC; (b) Camera f by Tsai; (c) Camera f by Zhang; (d) Projector f by Tsai-DLC configuration.

For the rest of parameters calculation and measurement error in Zhang method, a $\pm 5\%$ error was introduced in the parameters that interfere in the calculation of the camera calibration extrinsic parameters and a radial lens distortion of calibration Zhang method.

Also, it was observed that the camera calibration extrinsic parameters were substantially affected. Table 1 displays the average error and standard deviation that were obtained in the camera rotational and translational vector.

| | DLC | | TSAI | | ZHANG | |
|----------------|----------|-----------|---------|-----------|----------|-----------|
| | AVG. | STD DESV. | AVG. | STD DESV. | AVG. | STD DESV. |
| Tx (mm) | 3.115 | 2.018 | 6.4385 | 3.7526 | 2.812 | 1.482 |
| Ty (mm) | 2.731 | 2.4209 | 4.1095 | 2.7621 | 2.0214 | 2.0561 |
| Tz (mm) | 2.4103 | 0.6091 | 0.2308 | 1.4762 | 1.1203 | 0.8069 |
| Rx (°) | -0.007 | 0.2853 | 0.0031 | 0.1695 | 0.00004 | 0.00005 |
| Ry (°) | 0.0433 | 0.1291 | -0.0006 | 0.2118 | -0.00002 | 0.00002 |
| Rz (°) | -0.00006 | 0.00221 | 0.00001 | 0.00292 | -0.00001 | 0.00002 |

Table 1. Camera rotational and translational vector error

It is possible to see that the Tsai error in the translational vector is significantly higher for Tx and Ty but lower for Tz than the others. This is because Tsai method estimates Tz after determining the rest of the extrinsic parameters. The other methods estimate all the translation components at the same time. Meanwhile, concerning the rotation case, it was observed that the Zhang method was the least affected. This is because the method uses as a first approximation a DLT solution and the extrinsic parameters are determined after the intrinsic parameters have absorbed most of the error.

Table 2 displays the measurement error in the camera after introducing the previous mentioned error. It is important to remark that the measurement error is the key point to appreciate how the error spreads from camera parameters to measurement errors. These camera measurement errors obtained were considered the base error for each configuration because the projector was calibrated with a camera that had this starting measurement error.

Also, it was verified, by an Anderson–Darling test in MATLAB [39], that the statistical error distribution was a Gaussian.

| | DLC | | TSAI | | ZHANG | |
|---------------------|---------|------------|---------|------------|--------|------------|
| | AVG. | STD. DESV. | AVG. | STD. DESV. | AVG. | STD. DESV. |
| Error X (mm) | 0.0032 | 0.0179 | -0.1406 | 1.8390 | 0.0013 | 0.0003 |
| Error Y (mm) | -0.0015 | 0.0201 | -0.0297 | 0.8903 | 0.0011 | 0.0002 |

Table 2. Camera measurement error

The second part of this section shows the behavior of the different parameters shown in the first part but relative to the projector. It is important to remark that a projector without errors was simulated in order to appreciate only the influence of the camera on it.

The first parameter analyzed was focal length calculation. In the cases of DLC-DLC configuration and Zhang-DLC configuration, focal length calculation was no significant affected by the introduction of error in camera data. It was only in Tsai-DLC configuration that projector focal length calculation was affected. Figure 2 (d) shows the results of that. It is possible to appreciate that the distribution seen in the camera focal length was maintained in the projector focal length but with more dispersion.

As happened in the camera, the projector calibration extrinsic parameters were substantially affected. Table 3 displays the average error and standard deviation that were obtained in the projector rotational and translational vector. Again, it is possible to see that Tsai errors are significant higher that the obtained with DLC and Zhang.

| | DLC-DLC | | TSAI-DLC | | ZHANG-DLC | |
|----------------|----------|-----------|----------|-----------|-----------|-----------|
| | AVG. | STD DESV. | AVG. | STD DESV. | AVG. | STD DESV. |
| Tx (mm) | 2.291 | 2.1869 | 4.4819 | 4.0299 | 1.8514 | 1.519 |
| Ty (mm) | 1.6685 | 1.7936 | 3.2830 | 2.5822 | 1.6397 | 1.3422 |
| Tz (mm) | 0.8091 | 0.3004 | 0.2689 | 1.4488 | 0.9507 | 0.5461 |
| Rx (°) | 0.0037 | 0.1130 | 0.0031 | 0.1692 | 0.0002 | 0.0039 |
| Ry (°) | 0.0041 | 0.1380 | -0.0047 | 0.2108 | 0.0009 | 0.0019 |
| Rz (°) | -0.00001 | 0.00033 | 0.00006 | 0.00221 | -0.00001 | 0.00006 |

Tabla 3. Error de los vectores de rotación y traslación del proyector

As in the case of calibration extrinsic parameters, it was observed that the camera measurement error affected both the projector measurement error and camera-projector measurement error.

It is important to mention that the analysis of the different measurement errors gives us a clear vision of how the errors introduced in certain parameters of the camera first affect the measurement error of the camera, then of the projector (simulated without errors) and finally, of the entire system.

Table 4 displays average error and standard deviation obtained from the projector, originally without errors, after introducing the previous mentioned error and the one obtained in the camera-projector pair system. Subscript p is for projector and cp is for camera-projector.

Again, it was verified, by an Anderson–Darling test in MATLAB, that the statistical error distribution was maintained until the latest measurement error results [40]. The camera and camera-projector measurement error distribution of the three combinations maintained a Gaussian distribution.

| | DLC-DLC | | TSAI-DLC | | ZHANG-DLC | |
|-----------------------|---------|------------|----------|------------|-----------|------------|
| | AVG. | STD. DESV. | AVG. | STD. DESV. | AVG. | STD. DESV. |
| Error Xp (mm) | 0.0007 | 0.0098 | -0.1707 | 3.894 | 0.0003 | 0.0003 |
| Error Yp (mm) | -0.0007 | 0.0095 | -0.0573 | 2.7068 | 0.0002 | 0.0003 |
| Error Xcp (mm) | 0.004 | 0.0311 | -0.1613 | 3.8296 | 0.0015 | 0.0003 |
| Error Ycp (mm) | -0.0024 | 0.0282 | -0.0539 | 2.7098 | 0.0012 | 0.0003 |

Table 4. Projector and Camera-projector pair system measurement error after calibration

As may be observed, the Zhang-DLC configuration provided the smallest measurement error values. The camera-projector measurement error result is the combined effect of both sets of extrinsic parameters (camera and projector), therefore, some errors can be balanced with the others.

It is important to mention that the DLC method does not take into account distortions; therefore, it is recommending, after the calibration, to make some type of subsequent optimization, for example the bundle method [38] in order to improve obtained result.

4.- SYSTEM VALIDATION

The experimental tests were carried out with the same measuring equipment and setup before mentioned, Figure 1.

With this we cover the extrinsic parameters of the system. Since the intrinsic parameters of the SIDIO Pro unit are not public, the results of the self-calibration carried out by the SIDIO Pro unit will be used to replicate them in the CAM-PRO Simulator. The error is 0.007 mm in X axis, 0.006 mm in Y axis, 0.009 mm in Z axis, the average error is 0.015 mm and the standard deviation is 0.010 mm. The objective of the experimental tests for this section is validated the simulator developed by comparing the values obtained, with SIDIO Pro and the CAM-PRO Simulator, of the length error between two spheres and the shape error of one of these spheres, Figure 1.

While the distance between sphere center of the sphere bar pattern was 199.9943 mm, the distance between sphere center rebuilt by SIDIO Pro and CAM-PRO Simulator were 200.0986 mm and 200.0893 mm respectively.

Since the calculation of this length error is affected by the errors present in the reconstruction of the measured and simulated spheres, Table 5 shows the diameters and shape errors for the bar of standard spheres as well as those reconstructed by SIDIO Pro and by the CAM-PRO Simulator.

| | | Sphere bar pattern | Rebuilt by SIDIO Pro | Rebuilt by CAM-PRO Simulator |
|----------|------------------|--------------------|----------------------|------------------------------|
| Sphere 1 | Diameter (mm) | 24.9972 | 24.9879 | 24.9838 |
| | Shape error (mm) | 0.0017 | 0.0061 | 0.0054 |
| Sphere 2 | Diameter (mm) | 24.9961 | 24.9868 | 24.9799 |
| | Shape error (mm) | 0.0019 | 0.0070 | 0.0061 |

Table 5. Diameters and shape errors of the spheres.

Now, looking closely at Sphere 1, in Table 6 we can observe the average errors and its standard deviations obtained by SIDIO Pro and the CAM-PRO Simulator.

| | SIDIO Pro | CAM-PRO Simulator |
|-----------------|-----------|-------------------|
| Ave. Error (mm) | 2.4e-6 | 1.8e-6 |
| Std. Desv.(mm) | 0.0077 | 0.0076 |

Table 6. Sphere 1 errors obtained by SIDIO Pro and by the CAM-PRO Simulator.

As it is possible to observe, the values obtained by CAM-PRO Simulator are quite similar to the ones by SIDIO Pro, being possible to concluded that the Simulator CAM-PRO code is effectively valid, by having the necessary data, for simulations of specific situations with a measurement system formed by a camera and a projector.

5.- DISCUSSION

Numerous simulations were performed in MATLAB by the Monte Carlo method to characterize the behavior of measurement errors in a camera-projector pair, when they are calibrated separately. To understand the relationships between the camera and projector parameters better, and how uncertainty propagates from the camera to the projector, two error types were introduced. For DLC-DLC and Tsai-DLC configurations, a $\pm 5\%$ error was introduced in the camera data: dx , dy , C_u and C_v and a camera radial lens distortion coefficient $k_1=0.0015$. For Zhang-DLC configuration, a $\pm 5\%$ error was introduced in the parameters interfering in the calculation of the camera calibration extrinsic parameters and a camera radial lens distortion coefficient $k_1=0.0015$. All the errors mentioned before follow a normal Gaussian distribution.

Firstly, given the camera focal center results obtained, it can be seen that the calibration method most affected by the errors introduced for this calculation is DLC. Far from comparing to the other two methods, the dispersion shown in DLC focal center calculations is significant. Then, when the projector focal center calculation results were analyzed, the results obtained by DLC-DLC configuration and Zhang-DLC configuration were no significant affected. It was only in Tsai-DLC configuration that projector focal length calculation was affected and shown a direct relationship between camera and projector focal center calculations. The distribution seen in the camera focal length was maintained in the projector focal length but with more dispersion.

Also, it was possible to observe that in the other extrinsic parameters calculations, the Tsai-DLC configuration was again the most affected. It is clear therefore that Tsai method and every configuration that include this method are extremely sensitive to the variables dx , dy , C_u and C_v . Therefore, we recommend using Tsai method when it is sure that the camera parameters are accurate.

Secondly, with the base errors shown in Table 2, measurement errors in the camera, the projector was calibrated by DLC. And it was observed that projector calibration extrinsic parameters were affected and consequently the measurement errors of the camera-projector system. As we mentioned before, the camera-projector measurement error result is the combined effect of both sets of extrinsic parameters (camera and projector) that, therefore, some errors can be balanced with the others.

As was expected, the evidence seems to indicate that the Zhang-DLC configuration provides the smallest measurement error values. From the beginning, the camera calibration by Zhang method gave smaller errors in the extrinsic parameters and measurement results than the other methods. As we concluded before that Tsai method is the most sensitive method to the variables dx , dy , C_u and C_v that it was analyzed, it must therefore be recognizing that Zhang method is the least sensitive to them. Therefore, when it is not sure that the camera parameters are accurate we recommend to use Zhang method.

As we mentioned before, DLC method does not take into account the lens distortion and it is necessary, after the calibration, to make some type of subsequent optimization. It is recommended to use a bundle adjustment algorithm to improve DLC when there is no time limit to calculate the optimal solution, due to its high computational cost.

Finally, as has been verified after the validation of the CAM-PRO Simulator, it has satisfactorily simulated a specific real situation measured by the measuring equipment SIDIO Pro, being possible to conclude that the CAM-PRO Simulator code is valid.

REFERENCES

- [1] Buytaert, Jan and other. Aberration-free moire profilometry-Analysis, simulation and implementation of the optimal setup geometry in Optics and Lasers in Engineering, Agosto 2012, vol. 50, n° 8, p. 1119-1129, ISSN: 0143-8166, DOI: <http://doi.org/10.1016/j.optlaseng.2012.01.006>
- [2] Ribbens, Bart and other. Projection Moiré Profilometry Simulation Software for Algorithm Validation and Setup Optimisation in Optical measurement techniques for structures and systems 2 (OPTIMESS2012), Maastricht, by Shaker publishing, 2013, p. 349-358, ISBN 978-90-423-0419-2.
- [3] Mirza, Saba and Shaker, Chandra. Surface profiling of turbine blade using phase shifting Talbot interferometric technique in Proceedings of the SPIE: Interferometry XII: Applications, August 2004, Vol. 5532, p. 372-379, DOI: <https://doi.org/10.1117/12.560385>
- [4] Bieri, Louis-Severin and Jacot, Jacques. Three-dimensional vision using structured light applied to quality control in production line in Proceedings of the SPIE: Optical Metrology in Production Engineering, September 2004, Vol. 5457, p. 463-471, DOI: <https://doi.org/10.1117/12.545039>
- [5] Sadleir, Rosalind, Owens, Robyn and Hartmann, Peter. System for routine surface anthropometry using reprojection registration in Measurement science and Technology, 2003, Vol. 14, n° 11, p. 1912-1926, ISSN: 0957-0233, DOI: <http://doi.org/10.1088/0957-0233/14/11/009>
- [6] Sansoni, Giovanna, Trebeschi, Marco and Docchio, Franco. State-of-the-art and applications of 3D imaging sensors in industry, cultural heritage, medicine, and criminal investigation in Sensors, January 2009, Vol. 9, n° 1, p. 568-601, ISSN: 1424-8220, DOI: <http://doi.org/10.3390/s90100568>
- [7] Chen, Frank, Brown, Gordon and Song, Mumin. Overview of three-dimensional shape measurement using optical methods in Optical Engineering, January 2000, Vol. 39, n° 1, p. 10-22, ISSN: 0091-3286, DOI: <http://doi.org/10.1117/1.602438>
- [8] Schlobohm, Jochen, Pösch, Andreas and Reithmeier, Eduard. A raspberry pi base portable endoscopic 3D measurement system in Electronics, September 2016, Vol. 5, n° 3, article number 43, ISSN 2079-9292, DOI: <http://doi.org/10.3390/electronics5030043>
- [9] Zhang, Haolin and others. A systematic study and framework of fringe projection profilometry with improved measurement performance for in-situ LPBF process monitoring in Measurement, March 2022, Vol. 191, ISSN 0263-2241. DOI: <https://doi.org/10.1016/j.measurement.2022.110796>
- [10] Lui, Yue and others. A simple calibration method for a fringe projection system embedded within an additive manufacturing machine in Machines, September 2021, Vol. 9, n° 9, p. 200. DOI: <https://doi.org/10.3390/machines9090200>
- [11] Ghazouali, Safouane and others. Optimised calibration of machine vision system for close range photogrammetry based on machine learning in Journal of King Saud University - Computer and Information Sciences, June 2022, Vol. 34, n° 9, p. 7406-7418. ISSN 1319-1578. DOI: <https://doi.org/10.1016/j.jksuci.2022.06.011>.
- [12] Xia, Renbo and others. Detection method of manufacturing defects on aircraft surface based on fringe projection in Optik, April 2020, Vol. 208, ISSN 0030-4026. DOI: <https://doi.org/10.1016/j.jjleo.2020.164332>.
- [13] Xu, Jing and Zhang, Song. Status, challenges, and future perspectives of fringe projection profilometry in Optics and Lasers in Engineering, December 2020, Vol. 135, ISSN 0143-8166. DOI: <https://doi.org/10.1016/j.optlaseng.2020.106193>.
- [14] Santolaria, Jorge and other. Modelling and calibration technique of laser triangulation sensors for integration in robot arms and articulated arm coordinate measuring machines in Sensors, September 2009, Vol. 9, n° 9, p. 7374-7396, ISSN:1424-8220, DOI: <http://doi.org/10.3390/s90907374>
- [15] Brosted, Francisco and other. Laser triangulation sensor and six anthropomorphic robot manipulator modelling for the measurement of complex geometry products in Robotics and computer-integrated manufacturing, December 2012, Vol. 28, n° 6, p. 660-671, ISSN: 0736-5845, DOI: <http://doi.org/10.1016/j.rcim.2012.04.002>
- [16] Isa, Mohammed and others. Volumetric error modelling of a stereo vision system for error correction in photogrammetric three-dimensional coordinate metrology in Precision Engineering, April 2020, Vol. 64, p. 188-199, ISSN 0141-6359. DOI: <https://doi.org/10.1016/j.precisioneng.2020.04.010>.
- [17] Bender, Christoph and other. A Hand-held Laser Scanner based on Multi-camera Stereo-matching in Visualization of Large and Unstructured Data Sets: Applications in Geospatial Planning, Modeling and Engineering-Proceedings of IRTG 1131 Workshop 2011, Dagstuhl, by Schloss Dagstuhl-Leibniz-Zentrum fuer Informatik, 2012, p.123-133, ISBN: 978-3-939897-46-0, DOI: <http://doi.org/10.4230/OASlcs.VLUDS.2011.123>
- [18] Shammari, Ahmed and other. A Study to Evaluate the Calibration of Optical Three-Dimensional Scanner in Journal of Mechanical Engineering Research and Developments, February 2022, Vol. 44, n° 8, p. 359-370, ISSN: 1024-1752.
- [19] Dickin, Fraser, Pollard, Stephen and Adams, Guy. Mapping and correcting the distortion of 3D structured light scanners in Precision Engineering, June 2021, Vol. 72, p. 543-555. ISSN 0141-6359. DOI: <https://doi.org/10.1016/j.precisioneng.2021.06.001>.
- [20] Heikkila, Janne and Silven, Olli. A four-step camera calibration procedure with implicit image correction in Proceedings of IEEE Computer Society Conference on Computer Vision and Pattern Recognition, June 1997, p. 1106-1115, ISBN:0-8186-7822-4, ISSN: 1063-6919, DOI: <http://doi.org/10.1109/CVPR.1997.609468>
- [21] Tsai, Roger. An efficient and accurate camera calibration technique for 3D-machine vision in IEEE Conference on Computer Vision and Pattern Recognition (CVPR 86), ca. 1986, p. 364-374, ISBN: 9780818607219
- [22] Zhang Zhengyou. A flexible new technique for camera calibration in IEEE Transactions on Pattern Analysis and Machine Intelligence, November 2000, Vol. 22, n° 11, p. 1330-1334, ISSN:0162-8828, DOI: <http://doi.org/10.1109/34.888718>
- [23] An, Gwon Hwan and other. Charuco board-based omnidirectional camera calibration method in Electronics, December 2018, Vol. 7, n° 12, article number 421, ISSN 2079-9292, DOI: <http://doi.org/10.3390/electronics7120421>
- [24] Fraser, Clive. Photogrammetric camera component calibration: A review of analytical techniques in Calibration and Orientation of Cameras in Computer Vision of Springer series in information sciences book series, Germany, by Gruen & Huang, Springer-Verlag, 2001, Vol. 34, pp. 95-121, ISSN: 0720-678X, DOI: http://doi.org/10.1007/978-3-662-04567-1_4
- [25] Jantos, Ralf and other. Photogrammetric Performance Evaluation of the Kodak DCS Pro Back in Proceedings of the ISPRS commission V Symposium of International archives of photometry remote sensing and spatial information science, ca 2002, Vol. 34, n° 5, p. 42-47, ISSN: 1682-1750.
- [26] Peipe, Juergen and Stephani, Manfred. Performance evaluation of a 5 megapixel digital metric camera for use in architectural photogrammetry in International Archives of Photogrammetry Remote Sensing And Spatial Information Sciences, ca 2003, Vol. 34, n° 5, p. 259-261, <https://www.isprs.org/proceedings/XXXIV/5-W12/proceedings/65.pdf>
- [27] Läbe, Thomas and Förstner, Wolfgang. Geometric stability of low cost digital consumer cameras in Proceedings of the 20th International society for photogrammetry and remote sensing congress, Istanbul, 2004, Vol. 35, p. 528-535, ISSN 1682-1750, <https://www.isprs.org/proceedings/XXXV/congress/comm1/papers/95.pdf>

- [28] Kunii, Yoichi and Chikatsu, Hirofumi. On the application of 3 million consumer digital camera to digital photogrammetry in Videometrics and optical methods for 3D shape measurement of Proceedings of the society of photo-optical instrumentation engineers (SPIE), January 2001, Vol. 4309, p. 278-287, ISSN: 0277-786X, DOI: <https://doi.org/10.1117/12.410884>
- [29] Campanelli, Valentina, Howell, Stephen and Hull, Maury. Accuracy evaluation of a lower-cost and four higher-cost laser scanners in Journal of Biomechanics, January 2016, Vol. 49, n° 1, p. 127-131, ISSN 0021-9290. DOI: <https://doi.org/10.1016/j.jbiomech.2015.11.015>
- [30] Remondino, Fabio and Fraser, Clive. Digital camera calibration methods: considerations and comparisons in International Archives of the Photogrammetry, Remote Sensing and Spatial Information Sciences, 2006, Vol. 36, n° 5, p. 266-272. DOI: <http://doi.org/doi.org/10.3929/ethz-b-000158067>
- [31] Anwar, Hafeez. Calibrating projector flexibly for a real-time active 3D scanning system in Optik, 2018, Vol. 158, p. 1088-1094, ISSN: 0030-4026, DOI: <http://doi.org/10.1016/j.jileo.2018.01.005>
- [32] Feng, Xiuxia and other. The Comparison of Camera Calibration Methods Based on Structured-Light Measurement in Proceedings of DISP 2008: First international congress on image and signal processing, Sanya, by Li & Deng, May 2008, Vol. 2, p. 155-160, ISBN:978-0-7695-3119-9, DOI: <http://doi.org/10.1109/CISP.2008.163>
- [33] Zollner, Helmut and Sablatnig, Robert. Comparison of Methods for Geometric Camera calibration using Planar Calibration Targets in Proceedings of the 28th Workshop of the Austrian Association of Pattern Recognition, Graz, Österreich, by OCG Schriftenreihe, ca 2004, Vol. 28, p. 237-244, ISBN: 3-85403-179-3, <https://cvi.tuwien.ac.at/wp-content/uploads/2014/12/oagm04b.pdf>
- [34] Zhang, Xi and Zhang, Jian. Summary on calibration method of line-structured light sensor in 2017 IEEE International Conference on Robotics and Biomimetics, ca 2017, p. 1142-1147, ISBN:978-1-5386-3742-5, DOI: <http://doi.org/10.1109/ROBIO.2017.8324571>
- [35] Koppurapu, Sunil and Corke, Peter. The effect of noise on camera calibration parameters in Graphical Models, 2001, Vol. 63, n° 5, p. 277-303, ISSN 1524-0703, DOI: <https://doi.org/10.1006/gmod.2001.0551>
- [36] Martynon, Ivan, Kamarainen, Joni-Kristian and Lensu, Lasse. Projector calibration by inverse camera calibration in Lecture note in computer science of 17th Scandinavian conference (SCIA 2011), Ystad, by Heyden & Kahl, ca 2011, Vol. 6688, p. 536-544, ISBN: 978-3-642-21227-7, DOI: https://doi.org/10.1007/978-3-642-21227-7_50
- [37] Din, Irfanud Ud and other. Projector Calibration for Pattern Projection Systems in Journal of applied research and technology, February 2014, Vol. 12, p. 80-86, ISSN: 1665-6423, DOI: [http://doi.org/10.1016/S1665-6423\(14\)71608-6](http://doi.org/10.1016/S1665-6423(14)71608-6)
- [38] Huang, Junhui and other. Calibration of a camera-projector measurement system and error impact analysis in Measurement science and technology, December 2012, Vol. 23, n° 12, p. 14, ISSN: 0957-0233, DOI: <http://doi.org/10.1088/0957-0233/23/12/125402>
- [39] Anderson-Darling test – MATLAB adtest – MathWorks España [online] [consultation date: February 23, 2023]. Available in: <https://es.mathworks.com/help/stats/adtest.html>.
- [40] Furlan, Axel, Marzorati, Daniele and Sorrenti, Domenico. On the normality of the projection parameters in First interdisciplinary workshop on Mathematics of filtering and its applications (MFA2011), Contributed sessions, London, July 14th 2011.